Design of Organic Photovoltaics and Auxetic Networks

Daniel Reid, Nicholas Jackson, Nidhi Pashine, Sidney Nagel and Juan de Pablo

SOLUBILITY IN ORGANIC PHOTOVOLTAICS

INTRODUCTION

The light absorbing layer in organic photovoltaics (OPVs) consists of a finely interwoven network of two or more types of donor and acceptor molecules. For a device to achieve high efficiency, several challenges must be addressed: First, the donor and acceptor components must microphase separate, providing high interfacial area and conduits for charge transfer. Second, the microphases of donors and acceptors must connect to their respective electrodes. Third, the donor and acceptor must be designed such that they provide a high open-circuit voltage. The complex structures within the bulk heterojunction and the effects of these structures on the efficiency of OPV devices are poorly understood.

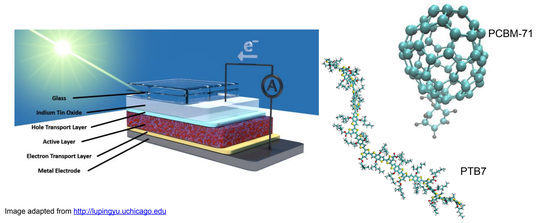

Image adapted from http://lupingyu.uchicago.edu

We model these systems at a variety of scales. At the finest level, we employ atomistic molecular dynamics to investigate local structure and solubility of the donor polymer PTB7 in a variety of solvents. We then systematically coarse-grain these atomistic models into a worm-like chain of ellipsoidal particles. Such models allow one to investigate larger length scales than possible in atomistic simulations. These models are iterated using a Monte Carlo formalism, allowing for complex rearrangements to be proposed, further enhancing equilibration. To address even larger length scales, we employ a particle-field representation. Here, we describe only mean-field interactions, considering the Flory-Huggins χ, as well as the orientational interactions of the polymers' pi systems and backbones. Using these models, we address length scales at which the bulk heterojunction manifests.

[1]M. B. Goldey, N. Brawand, M. Vörös, G. Galli. Under review.

SOLUBILITY PARAMETERS FROM SIMULATION

Control of aggregation during film formation is essential for the creation of efficient organic electronic devices. Solubility properties of these materials, however, are not well studied. We investigate the solubility behavior of PTB7 through two techniques. First, we determine the free energy of two PTB7 oligomers disassociating in solution. Results show that DIO promotes aggregation, making it a worse solvent.

Solubility parameters are broadly applicable compared to such free energy surfaces. We compute solubility parameters analogous to the Hansen solubility parameters for PTB7 and relevant solvents, finding good agreement with experiment. We also find that these solubility parameters predict solubilities in line with free energy calculations. We suggest that even though solubility parameters are shape-agnostic, such parameters apply to these systems.

	δ lit	δ sim	δd, sim	δe, sim	Ra (PTB7)
PTB7	None	18.0	17.5	4.3	N/A
CB	19.6[1]	19.8	19.3	4.4	3.7
DIO	18.8[1,2]	19.6	19.5	1.7	4.8
CN	20.7[1]	20.9	20.4	4.3	5.8
oDCB	20.5[3]	20.9	20.1	5.8	5.5
Toluene	18.2[3]	18.7	18.1	4.9	1.3

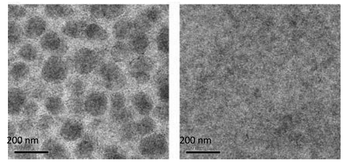

$$(Ra)^2 = 4(\delta_{d2} - \delta_{d1})^2 + (\delta_{e2} - \delta_{e1})^2$$

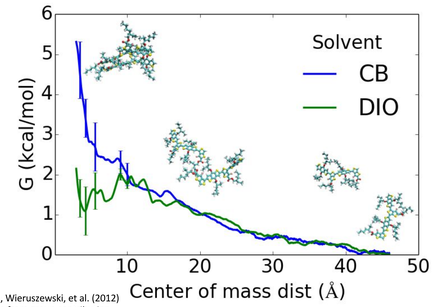

1. Graham, Wieruszewski, et al. (2012)
2. Estimate from group contribution theory
3. Hansen, Smith. Carbon (2004)

COARSE GRAINED MODELS

While atomistic models are instructive, they cannot address the scales necessary to model organic electronic films. We construct two progressively coarser representations which capture the anisotropic nature of conjugated polymers.

The first coarse grained polymer model consists of bonded Gay-Berne particles. The pi-pi stacking behavior of conjugated polymers is captured through the anisotropic nature of these particles.

The second model combines particle-continuum Monte Carlo polymer simulations with liquid crystal order parameters in order to capture both chain alignment and pi-pi stacking of conjugated polymer backbones.

These models take as an input the Flory-Huggins χ, which can be calculated from solubility parameters as determined from molecular dynamics simulations.

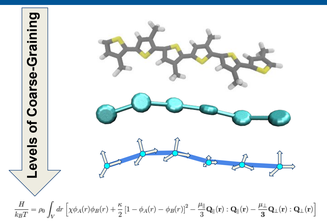

$$\frac{H}{k_B T} = \rho_0 \int_V d\mathbf{r} \left[\chi \phi_A(\mathbf{r}) \phi_B(\mathbf{r}) + \frac{\kappa}{2}[1 - \phi_A(\mathbf{r}) - \phi_B(\mathbf{r})]^2 - \frac{\mu_1}{3} \mathbf{Q}_1(\mathbf{r}) : \mathbf{Q}_1(\mathbf{r}) - \frac{\mu_2}{3} \mathbf{Q}_2(\mathbf{r}) : \mathbf{Q}_2(\mathbf{r}) \right]$$

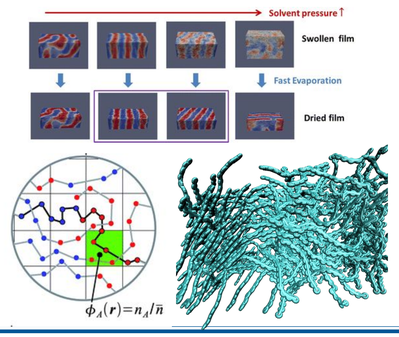

AUXETIC MATERIALS FROM AMORPHOUS NETWORKS

INTRODUCTION

Recent work has shown that disordered networks of nodes connected by bonds can be tuned to show a host of unusual properties. In disordered networks, global properties such as the Poisson's ratio, as well as local responses can be precisely tuned. Such networks with show promise in areas such as impact mitigation, mechanical fasteners, fabrics, filters, and in creating tailor-made mechanical responses. We create simulations which describe these networks as a set of points connected by harmonic springs with a weak bond-bending restraint parameterized to match the behavior of real materials. Using algorithms which selectively prune bonds, we lower the Poisson's ratio of these networks from their initial value of + 0.3 to - 0.6 after bond pruning. These finding are verified in experiment using laser-cut rubber configurations. By further modifying the strength of individual bonds, we further reduce the Poisson's ratio to - 0.725, with its lower limit being - 1.0.

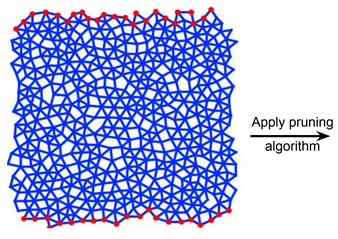

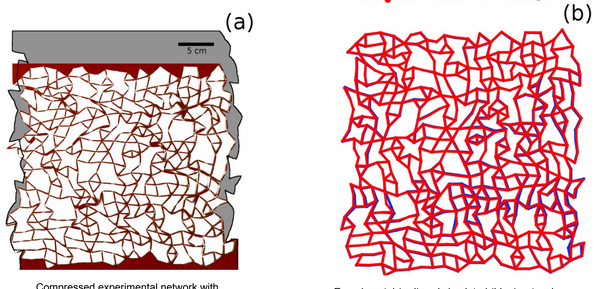

Compressed experimental network with original outline shown in grey

Experimental (red) and simulated (blue) network configurations at 3.1 % compression

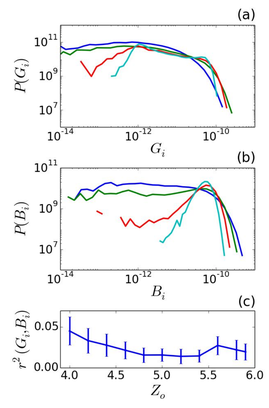

Probability distributions of bond responses for (Z=4.0, blue), (Z=4.8, green), (Z=5.4, red), (Z=5.9, teal)

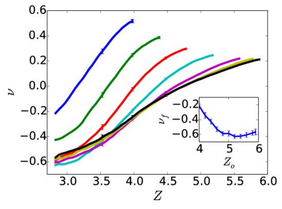

Poisson's ratio with pruning for networks with various initial coordination numbers

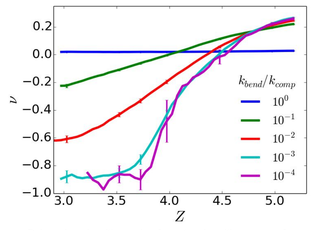

Poisson's ratio with pruning for networks with a range of bond bending strengths.

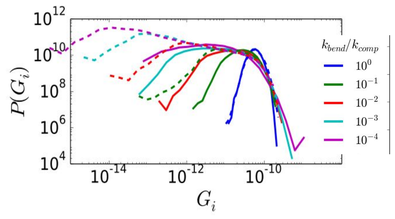

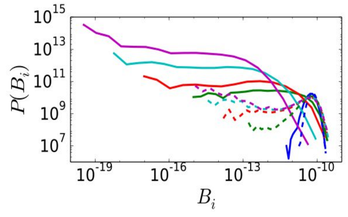

Stress distributions of bonds with varying bond bending strength before pruning (in dashed lines) and after pruning (in solid lines)